Tropical Journal of Pharmaceutical Research October 2020; 19 (10): 2129-2136
ISSN: 1596-5996 (print); 1596-9827 (electronic)

Available online at http://www.tjpr.org
http://dx.doi.org/10.4314/tjpr.v19i10.17

Original Research Article

Anti-proliferative activity of leaves of *Launaea capitata* Asteraceae: Phytochemical, cytotoxicity and in silico studies

Hany Ezzat Khalil[1,2]*, Turki Saeed Aldakheel[3], Anas AlAhmed[1], Promise Madu Emeka[1], Mahmoud Kandeel[4,5]

[1]Department of Pharmaceutical Sciences, College of Clinical Pharmacy, King Faisal University, Al-Ahsa 31982, [2]Department of Pharmacognosy, Faculty of Pharmacy, Minia University, Minia 61519, Egypt, [3]John Hopkins Aramco Healthcare, Dhahran, [4]Department of Physiology, Biochemistry and Pharmacology, College of Veterinary Medicine, King Faisal University, Al-Ahsa 31982, Saudi Arabia, [5]Department of Pharmacology, Faculty of Veterinary Medicine, Kafrelsheikh University, Kafr Elsheikh 33516, Egypt

For correspondence:* ***Email:* *heahmed@kfu.edu.sa;* ***Tel:*** *+966-563724624*

Sent for review: 25 May 2019 *Revised accepted: 24 September 2020*

Abstract

Purpose: *To investigate the phytochemical contents of Launaea capitata (L. capitate) and its potential cytotoxic activity. Also, to examine its molecular modeling by docking of the isolated compounds.*

Methods: *L. capitata was methanol-extracted and successively fractionated followed by determination of the total phenolic and flavonoid contents. Major constituents were isolated and purified. 3-(4, 5-Dimethyl-2-thiazolyl)-2,5-diphenyl-2H-tetrazolium bromide (MTT) cytotoxicity assays were conducted for all fractions. In silico studies were conducted using four anticancer target kinases, namely, protein kinase B (PKB/AKT), phosphatidylinositol 3-kinase (PI3K), protein kinase C (PKC), and rapidly accelerated fibrosarcoma kinases (RAFK).*

Results: *The results showed that total phenolic constituents ranged from 0.150 ± 0.004 to 60.229 ± 0.822 mg Gallic Acid Equivalent/g of dry extract, while the total flavonoid content varied from 0.004 ± 0.002 to 18.129 ± 1.599 mg quercetin equivalent/g of dry extract. Furthermore, the ethyl acetate fraction contained the highest amount of phenolic and flavonoid contents, which seemed to constitute the most effective anti-proliferative fraction. The plant's major constituent was apigenin-7-O-glycoside and was isolated from the ethyl acetate fraction. The MTT cytotoxicity assay revealed the anti-proliferative activity of ethyl acetate and butanol fractions, and apigenin-7-O-glycoside with half-maximal concentration (IC_{50}) comparable to that of doxorubicin. In silico studies revealed that apigenin-7-O-glycoside showed a better binding score and ligand efficiency when compared with standard ligands/inhibitors for AKT/PKB and PI3K, suggesting potential multiple targets for its anti-cancer activities.*

Conclusion: *L. capitata contains considerable amounts of phenolic and flavonoid components. Its major constituent, apigenin-7-O-glycoside is a potential lead compound for developing new anticancer compounds.*

Keywords: *Launaea capitata, Total phenolics, Total flavonoids, Docking, Cytotoxicity*

Tropical Journal of Pharmaceutical Research is indexed by Science Citation Index (SciSearch), Scopus, International Pharmaceutical Abstract, Chemical Abstracts, Embase, Index Copernicus, EBSCO, African Index Medicus, JournalSeek, Journal Citation Reports/Science Edition, Directory of Open Access Journals (DOAJ), African Journal Online, Bioline International, Open-J-Gate and Pharmacy Abstracts

INTRODUCTION

Cancer is a major health hazard and needs a continuous supply of new chemotherapeutic agents to combat its life-threatening nature. In this context, plant extracts and natural products remain the source of new chemotherapeutic agents. Family Asteraceae or Compositae is considered one of the largest flowering plant families, including more than 23,600 species and about 1,620 genera [1]. The genus *Launaea* belongs to the tribe Lactuceae (Cichorieae) of the family Compositae and represents about 40 species [2]. The Kingdom of Saudi Arabia has a huge and diverse body of flora, which contains about 2282 species in 855 genera [3]. *L. capitata* (Spreng.) Dandy (vernacular names: Hawa/Huwa), is a biennial herb widely distributed in the eastern part of the Arabian peninsula, including Saudi Arabia, Kuwait, and the United Arab Emirates [4].

L. capitata is an edible and refreshing herb used as a component in salad. From the literature few investigations have been done on the Egyptian and Qatari versions [2,5]; however, there have been no studies on the plant of Saudi origin. In addition, careful examination of the available literature revealed no studies on the phytochemical contents or medicinal activities of the plant's leaves.

Phenolic and flavonoid derivatives are important derivatives, with significant anticancer properties [3,6]. The molecular mechanisms associated with these compounds include apoptosis by inhibition of (PKB/AKT) [7], (PI3K) [8], (PKC) and (RAFK) [9].

As a result of the studies on the methanol extract of leaves of *L. capitata*, the current work reported the isolation and structural elucidation of apigenin-7-O-glycoside for the first time from the plant under investigation. Furthermore, this study examined the cytotoxic activity of different parts of the plant and apigenin-7-O-glycoside. In order to investigate the molecular bases of apigenin-7-O-glucoside activity, molecular modeling studies and docking runs were rigorously executed under internal co-crystalized ligand standards in comparison with known strong ligands or inhibitors for the protein targets AKT/PKB, PI3K, PKC, and RAFK2.

EXPERIMENTAL

General

The instruments and chemicals that were used included NMR spectra obtained using Bruker Avance III spectrometer (400 MHz). and Diaion HP-20 (Sigma Aldrich). Silica gel Column Chromatography (SCC) using silica gel 60-70-230 mesh (E. Merck, Germany). Reversed-Phase Silica Gel Column Chromatography (RPCC) was carried out on a Cosmosil 75C18-OPN (Nacalai Tesque, Japan; *internal diameter* = 50 mm, Length = 25 cm, with linear gradient: MeOH-H2O). Pre-coated silica gel 60 F_{254} plates, 0.25 mm in thickness (E. Merck; Germany). Visualization was done using 10 % solution of H_2SO_4 in ethanol, followed by drying and heating to 150 °C on a hot plate. The rest of the chemicals were purchased from Sigma Aldrich.

Plant material

L. capitata was collected from experimental station of King Faisal University, Al-Ahsa region (March 2018). The plant under investigation was authenticated by Dr. Mamdouh Shokry, Director of El-Zohria Botanical Garden, Giza, Egypt. A voucher specimen (no. 02-18-March -LC) of the plant was deposited in the Herbarium of the Department of Pharmaceutical Sciences, College of Clinical Pharmacy, King Faisal University, Al-Ahsa, Saudi Arabia.

Extraction and isolation of the plants major compounds

Air-dried leaves of *L. capitata* (700.0 g) were exhaustively extracted using cold maceration three times with methanol (MeOH) for 5.0 days using 5.0 L of 70.0 % MeOH at regular temperature and then concentrated under reduced pressure. The concentrated MeOH extract (59.0 g) was partitioned with n-hexane to yield n-hexane fraction (nHF) (26.0 g), and the remaining liquor was concentrated to give (33.0 g) defatted extract. The defatted extract (33.0 g) was subjected to partition with chloroform (6.0×250.0 mL). The obtained chloroform fractions (CHF) were also combined and concentrated into a semisolid mass (10.0 g), and both fractions were refrigerated in a strong-tight container. Likewise, ethyl acetate and n-butanol extracts were also obtained using the abovementioned method to yield an ethyl acetate fraction (EAF) (5.1 g) and n-butanol fraction (BTF) (3.0 g). The remaining aqueous fraction (AQF) (12.2 g) was freeze-dried and cooled for further use in an airtight container [10].

Ethyl acetate fraction (5.1 g) was subjected to Diaion HP-20 CC [150.0 g, H_2O (1.5 L) → MeOH (1.0 L) → acetone (3.0 L)] to give H_2O (1.3 g), MeOH (2.0 g) and acetone-eluted fractions (1.2 g) [11]. The MeOH-soluble fraction (2.0 g) was subjected to SCC [200.0 g, $CHCl_3$ (1.0

L)→$CHCl_3$-MeOH {[9:1(1.5 L)→7:3(1.0 L)→1:1(0.5 L)→3:7(0.5 L)] to yield seven fractions [Fr.1 (200.0 mg), Fr. 2(20.0 g), Fr. 3(400.0 g), Fr. 4(10.0 g), Fr. 5(300.2 mg), Fr. 6(30.0 g), Fr. 7(20..5 mg)]. Fr. 3 (400.0 mg) was separated by RPCC [100.0 g, MeOH-H_2O (2:3→1:1→3:2→7:3→4:1→9:1)→MeOH] to give compound (**1)** apigenin-7-O- glycoside (7.3 mg).

Total phenolic content determination

Total phenolic content estimation was done using the Folin-Ciocalteau index protocol [12]. Stock solutions of extracted fractions were prepared with the use of methanol (1 mg/mL). A half milliliter of the Folin-Ciocalteau reagent plus 6 mL of water were carefully added to 0.1 mL of each extract solutions. Furthermore, 1.5 mL of 20 % Na_2CO_3 solution plus water were added, making (10 mL). This was left for 2 hrs. Then after, the absorbance was measured at 760 nm. A Calibration curve was prepared by serially diluting the gallic acid in distilled water at concentrations of [0.5, 0.4, 0.3, 0.2 and 0.1 mg/mL, ($y = 0.903x + 0.0355$, $R^2 = 0.9471$)]. The total phenolic contents obtained, was presented as the equivalent of milligrams of gallic acid per gram of dried plant extract (mg GAE/g).

Total flavonoid content determination

Total flavonoid content was calculated according to the method of Khalil *et al* [13]. Ten milligrams of each of the stocked extracts were diluted with 100 mL of water and acetone at a 1:1 (v/v) ratio. Out of this, 0.25 mL was taken from each extract, and then 0.75 µL of 5 % (w/v) NaNO2, 0.15 mL of a freshly prepared10 % (w/v) aluminum chloride and 0.5 mL of 1 M NaOH solution were added, bringing a reaction mixture of 5 mL. The total volume then came to 10 mL with the addition of water. The reaction mixtures were kept for 5 minutes, and the absorption was read at 510 nm against the same reaction mixture lacking the sample. The calibration curve was prepared using quercetin as a reference standard in concentrations of 0.01, 0.02, 0.03, 0.04 and 0.05 mg/mL ($y = 0.0166x + 0.0007$, $R^2 = 0.9821$). The results obtained were represented as the equivalent of milligrams of quercetin per gram of dried plant extract (mg QE/g).

Cytotoxicity assay

The experiment was carried out using human lung cancer cell line (A549) and was obtained from the RIKEN Cell Bank, Japan, which is an adenocarcinoma human alveolar basal epithelial cell, and the viability was measured by the colorimetric MTT assay according to the method of Samy *et al* [14]. Doxorubicin (Wako, Japan) was used as a positive control. The cell growth inhibition (H) was calculated using Eq 1.

$$H\ (\%) = \{1- (AS - AB)/(AC - AB)\}100 \quad \ldots\ldots (1)$$

where AS is the absorbance of sample reaction mixture (contains all reagents and tested samples). AB is the absorbance of the blank reaction mixture (contains only test sample dissolved in DMSO). AC is the absorbance of the control reaction mixture (contains all reagents except for the test samples). IC_{50} was determined as the concentration of sample required to inhibit the formation of MTT formazan by 50 % [14].

Protein and ligand structures preparation

Retrieval of structure complexes, protein. and compounds preparation was performed as previously described with slight modifications [3]. Briefly, the protein data bank IDs 3CQW, 5UBR, 4RA4, and 5FD2 were used for AKT/PKB, PKC, PI3K, and RAFK, respectively. Docking was performed on structure-corrected, optimized, and energy-minimized structures. The structure of apigenin-7-O-glucoside, as well as the structures of standard inhibitors of the used proteins, were retrieved from PubChem database in 2D format. The 3D optimization of the compounds was performed using Ligprep software and saved as .sdf files.

Docking

The initial docking template was generated with Molegro software version 5.5, as previously described [3]. The energy grid resolution was kept as 0.3 Å and a grid radius of 10 - 15 Å. However, to ensure higher sampling efficiency, the MolDock scoring function was used after 20 numbers of runs of 1500 maximum iterations. The obtained docking results were compared to standard known inhibitors or modulators (reference compounds) specific to every protein (Table 1). In order to check the efficiency of docking procedures, redocking of the co-crystalized ligands was adopted. The obtained low RMSD from this experiment suggests the efficiency of the used docking protocol. To gain more insight into the analysis of the docking results, the lowest energy pose for every compound was used to estimate its ligand efficiency 1 (LE1) and ligand efficiency 3 (LE3) parameters as in Eqs 2 and 3, where the rerank scoring function is more computationally expensive in selecting the best pose from the resultant poses using the scoring function during the docking simulation.

LE1 = DS/HAC …… (2)

LE3 = RS/HAC …… (3)

where DS is the docking score. HAC is the heavy atom count. RS is the rerank score.

Statistical analysis

The data are presented as the means ± standard deviation (SD). Analysis was done with Excel graphics. IC_{50} was calculated using regression analysis.

RESULTS

Spectral characteristics of major compounds

The concentrated methanol extract was subjected to several chromatographic techniques to give several fractions and the flavonoid compound; apigenin-7-O- glucoside (**1**), (Figure 1). The structure was deduced by extensive inspection of spectroscopic data and comparison with reported values [15].

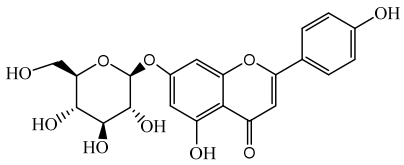

Figure 1: Structure of apigenin- 7-O-glucoside (**1**)

Total phenolic content

Total phenolic contents determination showed variation from one fraction to another and ranged from 0.150 ± 0.004 to 60.229 ± 0.822 mg GAE/g of dry extract (Figure 2). The results indicated that EAF had the highest percentage followed by BTF and AQF, in that order. CHF contained the least amount compared to EAF, while nHF showed very little phenolic content.

Total flavonoid content

The determination of total flavonoid content from various extracted fractions showed a similar trend observed from the total phenolic content determination. Contents varied from 0.004 ± 0.002 to 18.129 ± 1.599 mg QE/g of dry extract (Figure 2). Again, EAF showed the richest flavonoid content, followed by BTF, AQF, and CHF. The nHF content of flavonoids was insignificant.

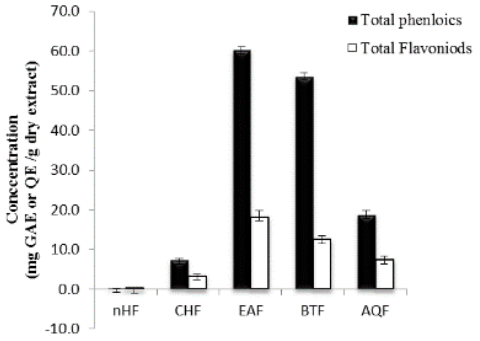

Figure 2: Total phenolic and flavonoid contents of different fractions of *L. capitata*. Data are the means ± standard deviation of three replicates

Cytotoxicity

The results of the MTT cytotoxicity assay on A549 cell line are shown in Figure 3. EAF, compound (**1**) and BTF showed comparable IC_{50}'s to the positive control, doxorubicin (43.1 µM). EAF was the most potent of the tested samples, as it showed the lowest IC_{50} (35.1 µg), followed by compounds (**1**) (64.3 µM) and butanol fraction (69.9 µg). nHF, CHF, and AQF showed very low IC_{50}.

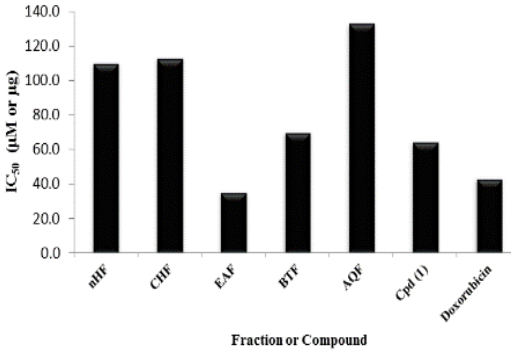

Figure 3: IC_{50} values of different fractions of *L. capitata* (µg) and compound (**1**) (µM) against the positive control (doxorubicin) (µM) using MTT assay on A549 cell line

Molecular modeling and docking scores

The docking score and docking pattern of apigenin-7-O-glucoside was evaluated and compared with standard known ligands for the tested target proteins. Apigenin-7-O-glucoside showed higher docking scores with AKT/PKB and PI3K compared with their standard ligands MK-2206 and wortmannin, respectively (Table 1). Additionally, among all protein targets, AKT/PI3K showed the highest docking score of -118. In contrast, the obtained docking scores suggested lower binding of apigenin-7-O-glucoside with PKC and RAF kinase.

Table 1: The docking scores of apigenin-7-O-glucoside with protein kinase B, phosphatidylinositol -kinase, protein kinase C, and rapidly accelerated fibro sarcoma kinase

Compound	AKT/PKB	PI3K	PKC	RAF kinase
Apigenin-7-O-glucoside	-118.0	-90.6223	-72.2838	-96.621
reference compound b	-94.4	-85.1324	-140.028	-101.101

[a]The score was calculated based on MolDock algorithm calculated by MVD. For every enzyme, a standard inhibitor was undertaken as a reference compound. A color scale was applied to identify the potency of compounds. The color ranging from red to blue implies lower to higher docking scores, respectively; [b] reference compounds: MK-2206 for AKT/PKB, Wortmannin for PI3K, Brostatin for PKC, and sorafenib for RAF kinase

In terms of ligand efficiency, L1 and L3 were analyzed for the tested compounds against AKT/PKB and PI3K, in which apigenin-7-O-glucoside showed improved ligand efficiencies (Table 2). Compared with the standard ligand, apigenin-7-O-glucoside showed 1.25- and 1.06-fold increase in L1 for AKT/PKB and PI3K, respectively. In consideration for reranking of the obtained poses, apigenin-7-O-glucoside showed improved L3 for PI3K by showing a 13-fold increase in L3 values over wortmannin. The rerank scoring for AKT/PKB docked poses implicated lower fractional L3 of 3-fold increase in L3 of apigenin-7-O-glucoside, compared with MK-2206.

Recognition of compounds into the binding site is derived by hydrogen bonds and stacking interactions as shown in figures (4 and 5).

DISCUSSION

The present study showed that the total flavonoids content was similar to those of total phenolic content, where EAF was the richest fraction in phenolic and flavonoid components; hence, these findings isolated and identified these components. This study led to the isolation of apigenin-7-O-glucoside.

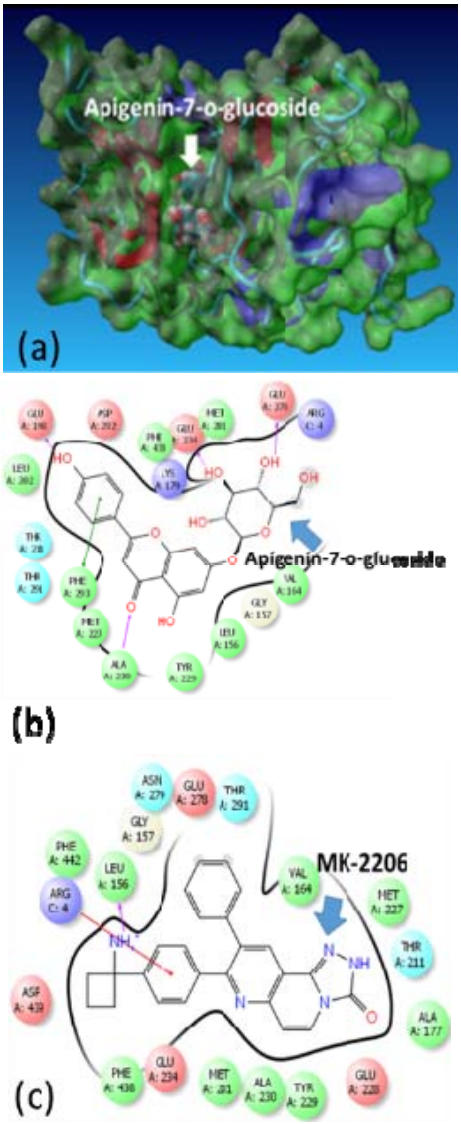

Figure 4: Schematic representation of AKT/PKB interactions with apigenin-7-O-glucoside and MK-2206: (**a**) Surface representation of AKT/PKB showing the docking site of apigenin-7-o-glucoside; (**b**) Ligand interaction diagram of apigenin-7-O-glucoside with AKT/PKB; (c) Ligand interaction diagram of MK-2206 with AKT/PKB. Purple arrow indicates hydrogen bonds with the backbone of protein. Dashed arrow indicates hydrogen bond with the side chains of residues. The direction of arrow is toward the acceptor site of hydrogen bonds.

Table 2: Hydrogen bonding, LE1 and LE3 parameters of the lowest energy pose of docking of apigenin-7-O-glucoside and MK-2206 with AKT/PKB and apigenin-7-O-glucoside and wortmannin with PI3K

Variable		H-Bond	LE1	LE3
AKT/PKB	Apigenin-7-O-glucoside	-15.91	-3.81	-2.42
	MK-2206	-2.50	-3.04	-0.71
PI3K	Apigenin-7-O-glucoside	-10.69	-2.92	-2.77
	wortmannin	-4.12	-2.75	-0.25

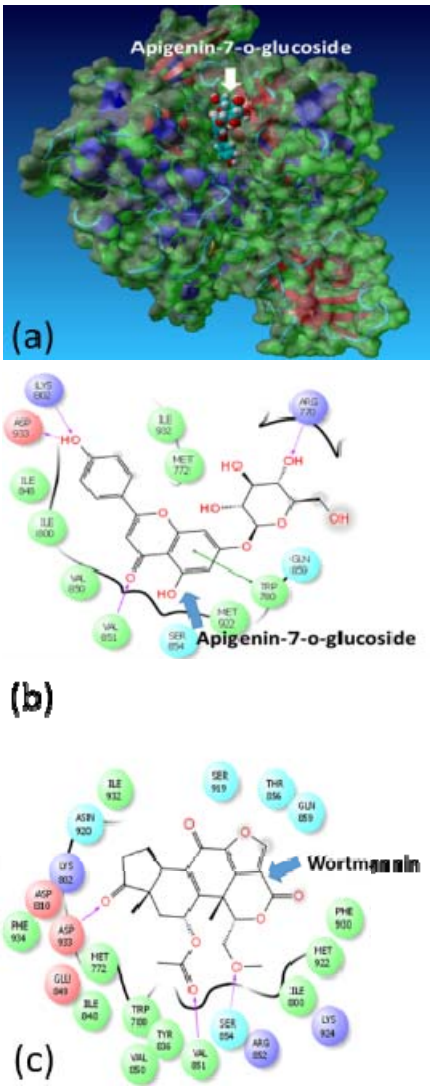

Figure 5: Schematic representation of PI3K interactions with apigenin-7-O-glucoside and wortmannin: (a) Surface representation of PI3K showing the docking site of apigenin-7-o-glucoside; (b) Ligand interaction diagram of apigenin-7-O-glucoside with PI3K; (c) Ligand interaction diagram of wortmannin with PI3K. Purple arrow indicates hydrogen bonds with the backbone of protein. Dashed arr**ow** indicates hydrogen bond with the side chains of residues. The direction of arrow is toward the acceptor site of hydrogen bonds.

The identity of the isolated compound was confirmed through comparison with previous literature using spectroscopic data.

The obtained cytotoxic effects of apigenin-7-O-glucoside suggest its potential use in the treatment of cancers. To gain more insight into the molecular mechanisms of apigenin-7-O-glucoside anti-proliferative activity, in-silico approaches were used to investigate its interaction with most of the common anti-cancer targets of phenolic and flavonoid compounds. Molecular modeling and docking have been used in the characterization of molecular targets, as well as virtual screening in drug discovery processes [16-18]. In this work, molecular modeling tools and docking investigations were performed to investigate the binding efficiency of apigenin-7-O-glucoside with four major targets in the treatment of cancers, AKT/PKB, PI3K, PKC, and RAFK. While apigenin-7-O-glucoside showed improved docking scores with AKT/PKB and PI3K, rerank scores suggested that PI3K is an expected target for apigenin-7-O-glucoside, as it sowed 13-folds higher L3 over wortmannin.

In order to analyze the changes associated with the improved ligand efficiencies of apigenin-7-O-glucoside, the contributing forces of ligand recognition were analyzed from the docking run output from Molegro software. In this context, there was a drastic increase in hydrogen bonding between apigenin-7-O-glucoside and AKT/PKB and PI3K, compared with the standard ligands (Table 2). Recognition of compounds into the binding site is derived by hydrogen bonds and stacking interactions. Figure 4a shows the docked ligands to the active site of AKT/PKB. Apigenin-7-O-glucoside showed a strong network of hydrogen bonds with AKT/PKB. Four hydrogen bonds with the side chains of GLU198 and GLU234 and the backbone of ALA230 and GLU278 support the binding of apigenin-7-O-glucoside with AKT/PKB. This network of hydrogen bonds is supported by stacking interaction of the phenol group with PHE293. In contrast, one hydrogen bond and stacking interaction with ARG4 were the detected ligand interactions of MK-2206.

Apigenin-7-O-glucoside showed two strong hydrogen atoms between its hydroxyl groups with the amino side chains of ARG770 and LYS802. These bonds are stronger than those produced with wortmannin`s oxygen and the carboxyl side chain of SER854 or the hydroxyl backbone of VAL851 or ASP933.

By analyzing the docked poses and ligand interactions, it is evident that the intrinsic power of apigenin-7-O-glucoside interaction with PI3K and AKT/PKB was supported by its phenolic group and hydroxyl moieties, which shares strong hydrogen bonds with the protein backbone and residue side chains.

The obtained docking profiles agree with previous findings. The highly related compounds luteolin and luteolin-7-O-glucoside were able to inhibit AKT/PKB and PI3K [19]. Additionally,

apigenin prevented human renal proximal tubular epithelial cells (HK-2) induced by cisplatin through interaction with AKT/PI3K pathway [20]. The concept of this study to target AKT/PKB is further supported by the previous finding that apigenin was able to inhibit the tumorigenic protein kinase protein in the Nano molar range [21]. In another study, apigenin-7-O-glucoside showed more potent cytotoxicity on HCT116 cells than apigenin [22]. This suggests that apigenin-7-O-glucoside may target AKT/PKB and PI3K during its anti-cancer activities.

According to cytotoxicity experiments and further insights from the molecular docking results, compound (**1**) could retain cytotoxic activities. The MTT cytotoxicity assay revealed that compound (**1**) had 62.8 % activity, compared to the used anticancer standard doxorubicin. These results are very promising, taking into consideration that compound (**1**) is considered natural and safe.

CONCLUSION

The results of this study indicate that *L. capitata* contains a considerable amounts of total phenolic and flavonoid components. Furthermore, the work has led to the isolation of apigenin-7-O-glucoside. Molecular docking data for the isolated compound show its activity on four enzymes directly related to cancer induction, thus suggesting that it possesses cytotoxic activity. *In vitro* cytotoxic results reveal the anti-proliferative activity of ethyl acetate fraction and apigenin-7-O-glucoside. Thus, the plant is a potential source of compounds for the treatment of cancer.

DECLARATIONS

Acknowledgement

The authors acknowledge the Deanship of Scientific Research at King Faisal University for the financial support under Nasher Track (Grant no. 186151).

Conflict of interest

No conflict of interest is associated with this work.

Contribution of authors

We declare that this work was done by the authors named in this article and all liabilities pertaining to claims relating to the content of this article will be borne by the authors.

REFERENCES

1. *Shahid M, Rao NK. First record of the two Asteraceae species from the United Arab Emirates. J New Biol Rep 2015; 4: 215-218.*
2. *Mansour RM, Ahmed AA, Saleh NA. Flavone glycosides of some Launaea species. Phytochemistry 1983; 22: 2630-2631.*
3. *Khalil HE, Mohamed ME, Morsy MA, Kandeel M. Flavonoid and Phenolic Compounds from Carissa macrocarpa: Molecular Docking and Cytotoxicity Studies. Phcog Mag 2018; 14: 304-310.*
4. *Norton J, Majid SA, Allan D, Al-Safran M, Böer B, Richer R. An illustrated checklist of the flora of Qatar; Browndown Publications: Gosport, UK, 2009; p 9.*
5. *Al-Easa HS. Fatty acids composition of Fifty-one plant species growing in Qatar. Int J Chem 2004; 14: 195-204.*
6. *Liu HL, Jiang WB, Xie MX. Flavonoids: recent advances as anticancer drugs. Recent Pat Anticancer Drug Discov 2010; 5: 152-164.*
7. *Granado-Serrano AB, Martín MA, Bravo L, Goya L, Ramos S. Quercetin induces apoptosis via caspase activation, regulation of Bcl-2, and inhibition of PI-3-kinase/Akt and ERK pathways in a human hepatoma cell line (HepG2). J Nutr 2006; 136: 2715-2721.*
8. *Soo HC, Chung FFL, Lim KH, Yap VA, Bradshaw TD, Hii LW, Tan SH, See SJ, Tan YF, Leong CO, et al. Cudraflavone C induces tumor-specific apoptosis in colorectal cancer Cells through inhibition of the phosphoinositide 3-kinase (PI3K)-AKT pathway. PLoS ONE 2017; 12: e0170551.*
9. *Fabbro D, Ruetz S, Buchdunger E, Cowan-Jacob SW, Fendrich G, Liebetanz J, Mestan J, O'Reilly T, Traxler P, Chaudhuri B, et al. Protein kinases as targets for anticancer agents: from inhibitors to useful drugs. Pharmacol Ther 2002; 93: 79-98.*
10. *Khalil HE, Aljeshi YM, Abdullah SF. Authentication of Carissa macrocarpa cultivated in Saudi Arabia; botanical, phytochemical and genetic study. J. Pharm Sci Res 2015; 7: 497-508.*
11. *Samy MN, Khalil HE, Sugimoto S, Matsunami K, Otsuka H, Kamel MS. Amphipaniculosides A–D, triterpenoid glycosides, and amphipaniculoside E, an aliphatic*

alcohol glycoside from the leaves of Amphilophium paniculatum. Phytochemistry 2015; 115: 261-8.

12. *Khalil HE, Aljeshi YM, Saleh FA. Phytochemical Analysis and in Vitro Antioxidant Properties of Sisymbrium irio L Growing in Saudi Arabia: A Comparative Study. Res J Pharm Biol Chem Sci 2017; 8: 2533-2540.*
13. *Khalil HE, Al-Ahmed A. Phytochemical Analysis and Free Radical Scavenging Activity of Carthamus oxyacantha Growing in Saudi Arabia: A Comparative Study. Int J Pharm Sci Rev Res 2017; 45: 51-55.*
14. *Samy MN, Khalil HE, Sugimoto S, Matsunami K, Otsuka H, Kamel MS. Biological studies on chemical constituents of Ruellia patula and Ruellia tuberosa. J Pharmacogn Phytochem 2015; 4: 64-67.*
15. *Moussaoui F, Zellagui A, Segueni N, Touil A, Rhouati S. Flavonoid constituents from Algerian L. resedifolia (OK) and their antimicrobial activity. Rec Nat Prod 2010; 4: 91–95.*
16. *Alnazawi M, Altaher A, Kandeel M. Comparative Genomic Analysis MERS CoV Isolated from Humans and Camels with Special Reference to Virus Encoded Helicase. Biol Pharm Bull 2017; 40: 1289-1298.*
17. *Kandeel M, Kitade Y. In silico molecular docking analysis of the human Argonaute 2 PAZ domain reveals insights into RNA interference. J Comput Aided Mol Des 2013; 27: 605-614.*
18. *Altaher Y, Kandeel M. Molecular analysis of some camel cytochrome P450 enzymes reveals lower evolution and drug-binding properties. J Biomol Struct Dyn 2016; 34: 115-124.*
19. *Park CM, Song YS. Luteolin and luteolin-7-O-glucoside inhibit lipopolysaccharide-induced inflammatory responses through modulation of NF-κB/AP-1/PI3K-Akt signaling cascades in RAW 264.7 cells. Nutr Res Pract 2013; 7: 423-429.*
20. *Ju SM, Kang JG, Bae JS, Pae HO, Lyu YS, Jeon BH. The flavonoid apigenin ameliorates cisplatin-induced nephrotoxicity through reduction of p53 activation and promotion of PI3K/Akt pathway in human renal proximal tubular epithelial cells. Evid Based Complement Alternat Med 2015; 2015: 1-9.*
21. *Duncan JS, Litchfield DW. Too much of a good thing: the role of protein kinase CK2 in tumorigenesis and prospects for therapeutic inhibition of CK2. Biochim Biophys Acta 2008; 1784: 33-47.*
22. *Smiljkovic M, Stanisavljevic D, Stojkovic D, Petrovic I, Vicentic JM, Popovic J, Grdadolnik SG, Markovic D, Sankovic-Babice S, Glamoclija J, et al. Apigenin-7-O-glucoside versus apigenin: Insight into the modes of anticandidal and cytotoxic actions. EXCLI journal 2017; 16: 795-807.*